Dalton Transactions

RSC Publishing

PAPER

View Article Online
View Journal | View Issue

Decomposition kinetics of peroxynitrite: influence of pH and buffer

Cite this: *Dalton Trans.*, 2013, **42**, 9898

Christian Molina, Reinhard Kissner and Willem H. Koppenol*

The decay of ONOOH near neutral pH has been examined as a function of isomerization to H^+ and NO_3^-, and decomposition to NO_2^- and O_2 *via* O_2NOO^-. We find that in phosphate buffer $k_{isomerization}$ = 1.11 ± 0.01 s^{-1} and $k_{disproportionation}$ = (1.3 ± 0.1) × 10^3 M^{-1} s^{-1} at 25 °C and I = 0.2 M. In the presence of 0.1 M tris(hydroxymethyl)aminomethane (Tris), the decay proceeds more rapidly: $k_{disproportionation}$ = 9 × 10^3 M^{-1} s^{-1}. The measured first half-life of the absorbance of peroxynitrite correlates with $[Tris]_0 \cdot ([ONOO^-]_0 + [ONOOH]_0)^2$, where the subscript 0 indicates initial concentrations; if this function exceeds 6.3 × 10^{-12} M^3, then Tris significantly accelerates the decomposition of peroxynitrite.

Received 9th April 2013,
Accepted 3rd May 2013

DOI: 10.1039/c3dt50945a

www.rsc.org/dalton

Introduction

Peroxynitrite† is formed from the reaction of NO˙ with $O_2^{\bullet-}$,[3] which proceeds at a diffusion-controlled rate, k = 1.6 × 10^{10} M^{-1} s^{-1}.[4,5] Because both NO˙ and $O_2^{\bullet-}$ are released by activated macrophages and neutrophils,[6–11] peroxynitrite can be formed *in vivo*.[12] Due to its oxidizing power and nitrating activity, peroxynitrite is cytotoxic and is associated with inflammatory diseases.[13]

$ONOO^-$ is stable in a cold alkaline solution in the absence of carbonyl compounds and metals. The pK_a of ONOOH increases from 6.5 to 7.3 with increasing phosphate concentration.[14] Isomerization of ONOOH to HNO_3,[15,16] reaction 1,‡ is first-order in ONOOH. Rate constants for the isomerization, obtained over a period of *ca.* 40 years, have slightly decreased, from 1.5 to 1.1 s^{-1}, most likely because of purer preparations of peroxynitrite (Table 1). ONOOH is a powerful one-electron and two-electron oxidant.[17,18] A review of the literature shows that evidence for the much-cited homolysis of ONOOH to HO˙ and $NO_2^{\bullet}$ is weak: at most 5% of ONOOH may undergo this reaction.[19] In any case, the reaction of otherwise stable $ONOO^-$ with CO_2 [20] is far more relevant to biology (k = (3–5.8) × 10^4 M^{-1} s^{-1})[21,22] as it yields, in part, very oxidising species, $NO_2^{\bullet}$ and $CO_3^{\bullet-}$ with $E^\circ(NO_2^{\bullet}/NO_2^-)$ = 1.04 V[23] and $E^\circ(CO_3^{\bullet-}/CO_3^{2-})$ = 1.59 V.[24] These species are responsible for the higher yield of nitration of phenols compared to nitration by peroxynitrite alone (4–9% without and 14–19% with 20 mM HCO_3^-).[22,25–27]

Deviations from first-order behaviour[33] and formation of O_2 [34] and NO_2^- in a 1 : 2 stoichiometric ratio[35] have been observed. Both phenomena can be explained with an additional reaction, namely between ONOOH and $ONOO^-$, a disproportionation that, given a pK_a of ONOOH of nearly 7, is only relevant near and above neutral pH (Scheme 1). This disproportionation thus fits the observation that NO_2^- yields increase with pH and with peroxynitrite concentration.[36,37] Gupta *et al.*[38] showed that the disproportionation reaction

Table 1 The literature values for rate constant k_1 of the isomerization of ONOOH at 25 °C

Year	Reference	k_1/s^{-1}	Remarks
1970	28	1.5	*a,b*
1990	12	0.65 ± 0.05	*a,c*
1992	17	1.3	*a*
1993	29	1.0 ± 0.2	*a*
1997	30	1.25	*a*
1997	14	1.20	I = 0.2 M
1998	31	1.20	I = 0.1 M
2003	32	1.10 ± 0.05	I = 0.9 M
2012	This work	1.11 ± 0.01	I = 0.2 M

[a] Ionic strength is not given. [b] At r.t. [c] At 37 °C.

Institute of Inorganic Chemistry, Department of Chemistry and Applied Biosciences, ETH Zurich, 8093 Zurich, Switzerland. E-mail: koppenol@inorg.chem.ethz.ch

†"Peroxynitrite" refers to a mixture of $ONOO^-$ and ONOOH, depending on the pH; "peroxynitrate" refers to a mixture of O_2NOO^- and O_2NOOH, depending on the pH. Buffers: Tris, tris(hydroxymethyl)aminomethane; Hepes, 2-[4-(2-hydroxyethyl)piperazin-1-yl]ethanesulfonic acid; Pipes, 1,4-piperazinediethanesulfonic acid. Formulae, trivial names and systematic names: $ONOO^-$, peroxynitrite, (dioxido)oxidonitrate(1−); ONOOH, peroxynitrous acid, (hydridodioxido)oxidonitrogen; O_2NOO^-, peroxynitrate, (dioxido)dioxidonitrate(1−); O_2NOOH, peroxynitric acid, (hydridodioxido)dioxidonitrogen; NO˙, nitric oxide, oxidonitrogen(˙) or nitrogen monoxide; $O_2^{\bullet-}$, superoxide, dioxide(˙1−) or dioxidanidyl; HNO_3, nitric acid, hydroxidodioxidonitrogen; HO˙, hydroxyl, hydridooxygen(˙) or oxidanyl; $NO_2^{\bullet}$, pernitric oxide, nitrogen dioxide or dioxidonitrogen(˙); CO_2, carbon dioxide, dioxidocarbon; $CO_3^{\bullet-}$, trioxidocarbonate(˙1−); CO_3^{2-}, carbonate, trioxidocarbonate(2−); HCO_3^-, hydrogencarbonate, hydridooxidodioxidocarbonate(1−); NO_2^-, nitrite, dioxidonitrate(1−); O_2, dioxygen; H_2O_2, hydrogen peroxide or dioxidane.[1,2]

‡Reactions 1–5 are part of Scheme 1.

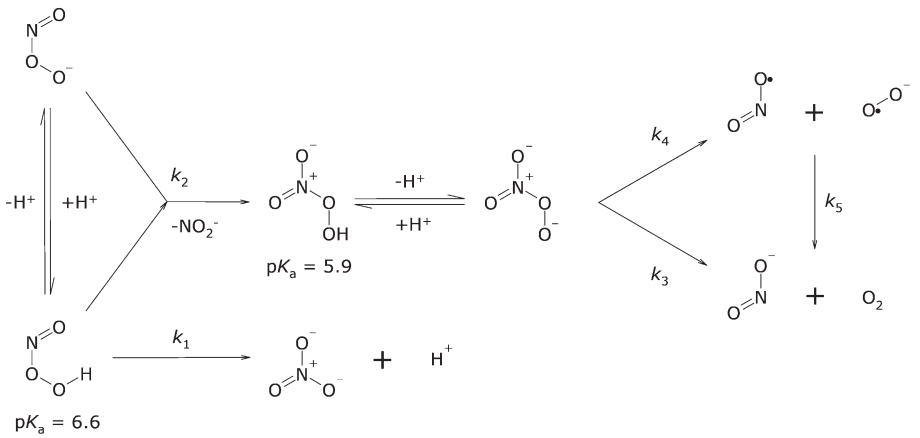

Scheme 1

yields initially O_2NOO^- and NO_2^-. O_2NOOH has a pK_a of 5.9[39,40] and is relatively stable. When one compares the wavelengths of maximal absorptivity and the extinction coefficients of $ONOO^-$ and O_2NOO^-, one sees that these parameters are quite similar: O_2NOO^- absorbs with ε_{max} = 1650 M^{-1} cm^{-1} at 285 nm,[39] and $ONOO^-$ with ε_{max} = 1705 M^{-1} cm^{-1} at 302 nm.[41] Furthermore, the rates of decay of both ONOOH and O_2NOO^- are close to 1 s^{-1} (see below). For these reasons O_2NOO^- went unnoticed as an intermediate during the decay of peroxynitrite. The decomposition of O_2NOO^- yields NO_2^- and O_2,[39] of which *ca.* 1–2% is in an excited ($^1\Delta_gO_2$) state.[42] Estimates for decomposition reaction 3 at 25 °C are k_3 = 1.0 ± 0.2 s^{-1},[39] 1.35 ± 0.03 s^{-1},[43] and 0.58 s^{-1}.[38] k_4 and k_{-4} are estimated to be 1.05 ± 0.23 s^{-1} [43] and (4.5 ± 1.0) × 10^9 M^{-1} s^{-1},[39] respectively. Redox reaction 5 is thermodynamically favoured, $\Delta_{rxn5}G^{o\prime}$ = −118 kJ mol^{-1}. Δ_fG^0 (kJ mol^{-1}) values in aqueous solution are 62.5 for $NO_2^{\bullet}$,[44] 33.8 for $O_2^{\bullet-}$,[45] −38 for NO_2^- [23,44] and 16.4 for O_2;[46] the reaction proceeds with k_5 = 1 × 10^8 M^{-1} s^{-1}.[47] We emphasise that the formation of O_2NOO^-, a reaction that is second-order in peroxynitrite, is biologically insignificant, because the concentration of peroxynitrite that may be generated by activated macrophages is very low. However, upon bolus additions of peroxynitrite during *in vitro* experiments that result in initial concentrations exceeding 0.1 mM, the formation of peroxynitrate should be taken into account.

In neutral 0.1 M tris(hydroxymethyl)aminomethane (Tris) buffer, decomposition of peroxynitrite yields up to 40% peroxynitrate with k_2 = 3 × 10^4 M^{-1} s^{-1}.[38] Decomposition of peroxynitrite in various neutral amine buffers, *e.g.* 2-[4-(2-hydroxyethyl)-piperazin-1-yl]ethanesulfonic acid (HEPES) or 1,4-piperazine-diethanesulfonic acid (PIPES), yields an oxidant that was suggested to be H_2O_2.[48] However, it could well have been O_2NOOH. The pH of peroxynitrite containing samples is usually controlled by phosphate buffer, and rarely by Tris or HEPES buffer (*e.g.* ref. 49 and 50). At equal pH, similar initial peroxynitrite concentrations yield more NO_2^- in Tris buffer[50] than in phosphate buffer.[36] This indicates that a Tris-dependent conversion of peroxynitrite to NO_2^- takes place. The possibility that the buffer influences the course or result of a reaction has rarely been considered.[48,51] We therefore also compared decomposition kinetics of peroxynitrite at pH = 6.8 in buffers that contain variable concentrations of phosphate and Tris and refined the decomposition model by taking into account reactions (1)–(3).

Materials and methods

Materials

$(Me_4N)OONO$ was prepared according to the work by Bohle *et al.*,[52] dissolved in 0.01 M NaOH and frozen as 25 mM solutions. $NaH_2PO_4{\cdot}H_2O$ (s), $Na_2HPO_4{\cdot}12H_2O$ (s), $H_2NC(CH_2OH)_3$ (s), NaOH (s), 85% H_3PO_4 (aq), and 70% $HClO_4$ (aq), all of analytical grade, were purchased from Sigma-Aldrich/Fluka (Buchs, CH), Brenntag Schweizerhall AG (Basel, CH), Merck (Darmstadt, DE), Riedel-de Haën (Seelze, DE) and used as received. Ar and N_2, both of 99.995% purity, were taken from the in-house gas supply. All solutions were prepared in deionized water that was further purified by using a Milli-Q unit from Millipore AG (Zug, CH).

Preparation of solutions

All solutions were prepared, stored, transferred and mixed at room temperature in glass vessels under Ar or N_2 and used within one day. Because $ONOO^-$ is sensitive to acid, heat and light, samples (1.4 g) of deeply frozen 25 mM $(Me_4N)OONO$ (aq) were dissolved in ice-cold 20 mM aqueous NaOH to produce alkaline $ONOO^-$ solutions that were stored and transferred at 0 °C and kept in the dark. The fresh alkaline $ONOO^-$ solutions contained $ONOO^-$, NO_2^- and NO_3^- in a molar ratio of 10 : 1 : 1 (see the section 'Determination of peroxynitrite, nitrite and nitrate'). The impurity by NO_2^- and NO_3^- in the alkaline $ONOO^-$ solutions is most probably formed during the thawing of frozen $(Me_4N)OONO$ (aq).[53] Because the pK_a of ONOOH depends on the ionic strength of the medium,[14] the ionic strength of the Tris buffers and the pH-varied 0.07 M phosphate buffers was adjusted to 0.2 M by the addition of $NaClO_4$, which we assume to be inert. Considering the

ion-pairing of Na^+ with HPO_4^{2-},[54] we calculated the ionic strength of our samples at pH 6–8 to be between 0.197 M and 0.206 M. The pK_a of ONOOH is 6.7 under these conditions.

Determination of peroxynitrite, nitrite and nitrate

The content of peroxynitrite and of its typical ionic decomposition products – NO_2^- and NO_3^- – were quantified for the lot of deeply frozen $(Me_4N)OONO$ (aq) used for kinetics experiments as described before.[36] Briefly, a sample (1.4 g) of deeply frozen $(Me_4N)OONO$ (aq) was subsequently weighted, dissolved in ice-cold 2 mM NaOH and analysed by spectrophotometry at 302 nm (Specord 250 from Analytik Jena AG, Jena, DE). To determine the content of NO_2^- and NO_3^-, a sample (1.4 g) of deeply frozen $(Me_4N)OONO$ (aq) was dissolved in 30 ml ice-cold 2 mM NaOH. 1 ml of this alkaline solution was added to 5 ml ice-cold 2 mM phosphoric acid to yield a mixture with pH = 3. In an acidic solution, peroxynitrite is mainly present as ONOOH, which isomerises to NO_3^-. This acidic solution was neutralised after 5 min by the addition of 4 ml 2 mM NaOH and then analysed by ion chromatography (Super Sep IC Anion Column from Metrohm AG, Herisau, CH) with a phthalate eluent of pH = 4.7 and by conductometric detection (732 IC Detektor from Metrohm AG, Herisau, CH). To determine the content of NO_3^- in the $(Me_4N)OONO$ (aq) sample, the peroxynitrite content was subtracted from the content of NO_3^-, which resulted after isomerization of ONOOH. The amount of peroxynitrate was not determined because it decays very fast in an alkaline medium.

Stopped-flow experiments

The decay of peroxynitrite was initiated by a rapid 1 : 1 mixing of an alkaline $ONOO^-$ solution with an acidic buffer solution in a thermostated (25 °C) stopped-flow unit (SX17MN) from Applied Photophysics (Leatherhead, UK) and observed for 10 s by spectrophotometry. Monochromatic light at the absorption maximum of $ONOO^-$, 302 nm, was used.

For each sample the decay of the absorption was measured at least four times, and the decay traces were averaged before analysis. The initial absorption of each mixture was used to calculate $[ONOO^-]_0$: the optical path length is 1 cm, and $\varepsilon_{302\ nm}(ONOO^-) = 1705\ M^{-1}\ cm^{-1}$.[41]

Prior to each decay experiment, the total initial peroxynitrite concentration in the sample, $[ONOO^-]_{0,\,total}$, was derived from the absorbance of a 1 : 1 mixture of an alkaline $ONOO^-$ solution with 20 mM NaOH. Then the experiments were carried out at the desired pH in a specific buffer. Prior to switching to another pH and buffer, the standardization with NaOH was repeated. For each mixture, the final pH value was measured by an Orion Microprocessor Ionalyzer 901 from Thermo Scientific after mixing, outside the stopped-flow apparatus. For the decay simulations, the pK_a of ONOOH was calculated from the measured pH, $[ONOO^-]_0$ and $[ONOO^-]_{0,\,total}$ at pH = 6.8.

Computations

We assume that at pH < 6 ONOOH isomerises to NO_3^- and H^+ exclusively; the decay of ONOOH was fitted to a single exponential function that resulted in k_{obs}. The rate constant k_1 was derived from k_{obs}, which is a function of pH, p$K_{a(ONOOH)}$ and k_1:

$$k_{obs} = k_1 \frac{[H^+]}{[H^+] + K_{a(ONOOH)}} \rightarrow k_1 = k_{obs}\left(1 + \frac{K_{a(ONOOH)}}{[H^+]}\right) \quad (1)$$

Reactions (1)–(3)§ lead to rate laws 2 and 3 for peroxynitrite and peroxynitrate.

$$\frac{\partial[ONOO^-]_{total}}{\partial t} = -k_1[ONOOH] - 2k_2[ONOOH][ONOO^-] \quad (2)$$

$$\frac{\partial[O_2NOO^-]_{total}}{\partial t} = k_2[ONOOH][ONOO^-] - k_3[O_2NOO^-] \quad (3)$$

Given the pK_a values of ONOOH and O_2NOOH, we calculated the time-dependent concentrations of the absorbing species $ONOO^-$ and O_2NOO^-.

$$\frac{\partial[ONOO^-]}{\partial t} = -k_1 \frac{[H^+][ONOO^-]}{[H^+] + K_{a(ONOOH)}} - 2k_2 \frac{[H^+][ONOO^-]^2}{[H^+] + K_{a(ONOOH)}} \quad (4)$$

$$\frac{\partial[O_2NOO^-]}{\partial t} = k_2 \frac{K_{a(O_2NOOH)}[H^+][ONOO^-]^2}{\left([H^+] + K_{a(O_2NOOH)}\right)\left([H^+] + K_{a(ONOOH)}\right)} - k_3 \frac{K_{a(O_2NOOH)}[O_2NOO^-]}{[H^+] + K_{a(O_2NOOH)}} \quad (5)$$

With the extinction coefficients [$\varepsilon_{302\ nm}(ONOO^-) = 1705\ M^{-1}\ cm^{-1}$; $\varepsilon_{302\ nm}(O_2NOO^-) = 1370\ M^{-1}\ cm^{-1}$ from the spectrum in ref. 38], we reproduced the absorption trace of peroxynitrite solutions at 302 nm. The calculated absorbance trace was fitted to the measured absorbance trace by the variation of the rate constants according to the method of the least squares. All data analysis and model calculations were carried out in Microsoft Excel by macro programmes (which are available from the authors upon request). The kinetics of the mixed-order decomposition of peroxynitrite was quantitatively compared by the use of the first half-life of the absorbance.

Results

Computation of the decomposition rate constants of peroxynitrite in phosphate buffer

From the measurement of the initial absorbance at various pH values, we derive a p$K_{a(ONOOH)}$ of 6.7 at I = 0.2 M which fits with the dependence of the pK_a on ionic strength.

A rate constant $k_1 = 1.11 \pm 0.01\ s^{-1}$ (n = 7, 95% confidence level) was determined by fitting absorbance traces at pH = 5.3 and I = 0.2 M in 70 mM phosphate buffer (see Fig. 1). At this pH, $[ONOO^-]$ is too low to contribute to significant

§ Reactions 1–5 are part of Scheme 1 with correspondingly numbered rate constants.

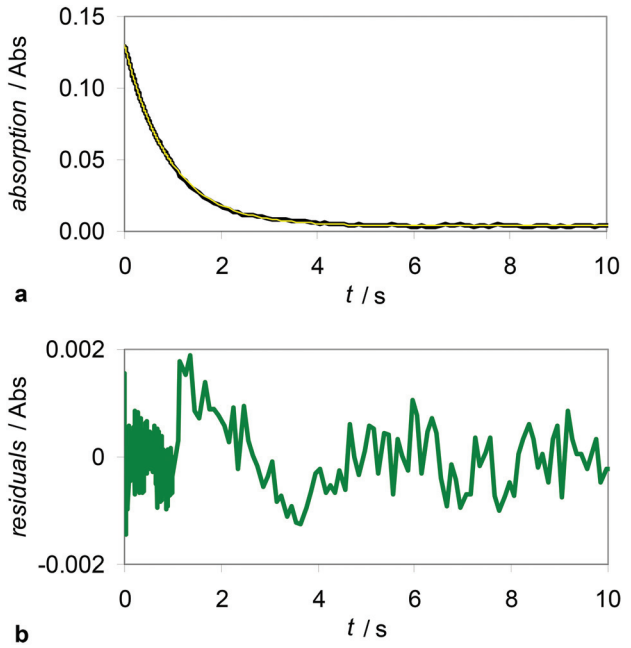

Fig. 1 Decomposition of 0.25 mM peroxynitrite at 25 °C and pH = 5.3 in 0.07 M phosphate buffer (I = 0.2 M) and simulation according to isomerization only with k_1 = 1.11 s^{-1}. (a) Actual decay curve measured (black) and simulated (yellow); (b) residuals (green) of the model.

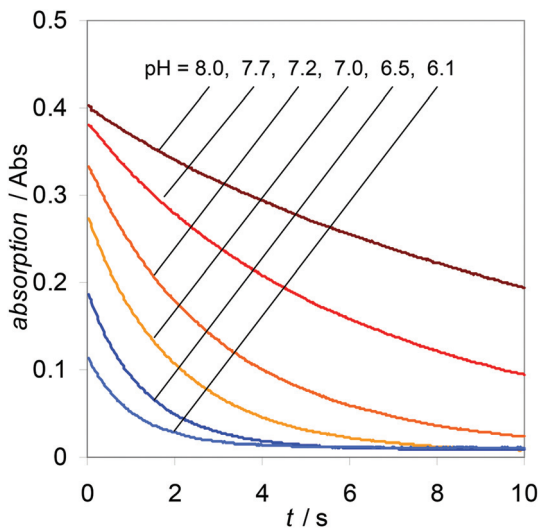

Fig. 2 Four to six decay traces per pH value (0.25 mM peroxynitrite in 70 mM phosphate buffer at 25 °C and I = 0.2 M, see Table 2) were measured at 302 nm and averaged.

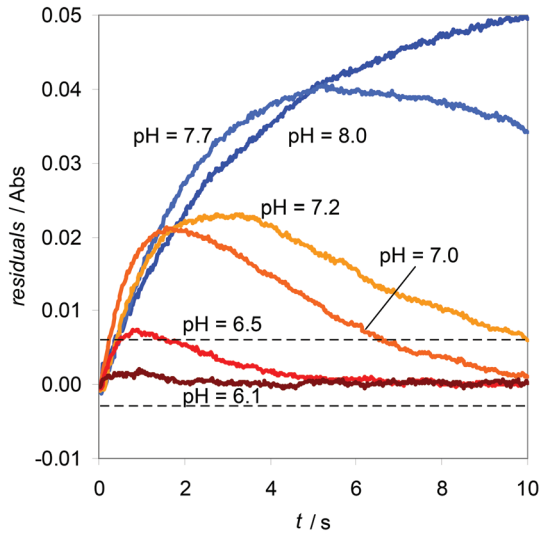

Fig. 3 Four to six decay traces per pH value (0.25 mM peroxynitrite in 70 mM phosphate buffer at 25 °C and I = 0.2 M, see Table 2) were averaged and fitted with k_1 = 1.11 s^{-1}. The residuals are much larger than in Fig. 4, the range of which is indicated by the two dashed lines.

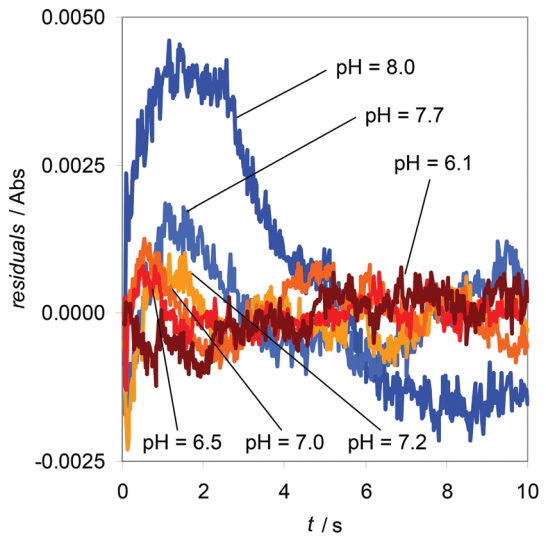

Fig. 4 The same as Fig. 3, but fitted with k_1 = 1.11 s^{-1} and k_3 = 1.35 s^{-1}.[43] k_2 was varied to minimise the residuals shown here.

disproportionation, and [HNO_2], from the nitrite present in the (Me_4N)OONO preparation, is too low to cause undesired reactions.

It became clear that the results obtained at higher pH (Fig. 2) could not be fitted with k_1 = 1.11 s^{-1} (Fig. 3). We therefore take into account an additional process, disproportionation of peroxynitrite to O_2NOO^- and NO_2^-.[38] For the decay of O_2NOO^- to NO_2^- and O_2, we take a value of 1.35 s^{-1}.[43] The combination of these three processes allows us to fit the obtained results with significantly smaller errors (Fig. 4).

Fig. 5 shows an actual decay curve of 0.25 mM peroxynitrite at pH = 6.5 which was fitted according to rate laws 2 and 3 with k_1 = 1.11 s^{-1} and k_3 = 1.35 s^{-1}.[43] In addition, the fit required that k_2 be 1163 M^{-1} s^{-1}: the residuals are very small and do not show any systematic error. This procedure was repeated at various other pH values, and the results for k_2 are presented in Table 2.

The first half-life of the absorbance increases with pH (Fig. 6) because $ONOO^-$ is stable and the isomerization of ONOOH is the predominant decomposition pathway of

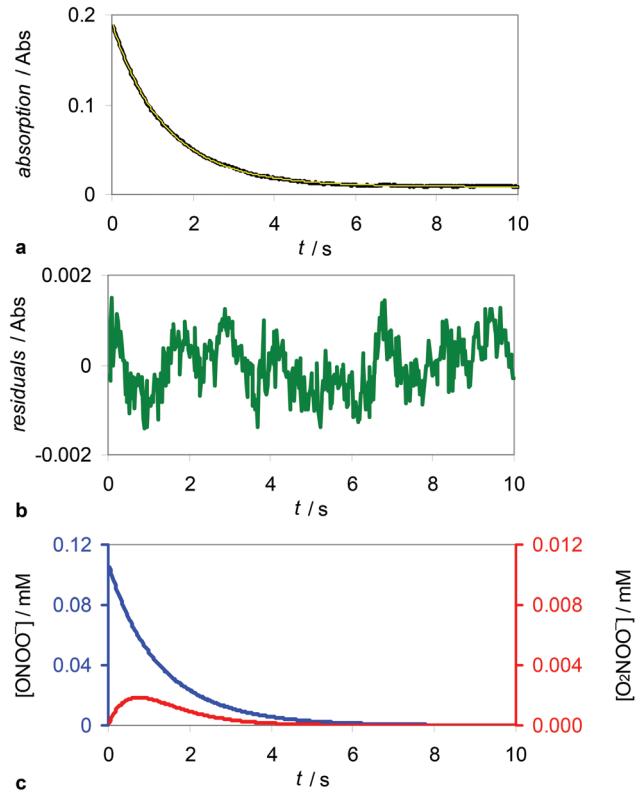

Fig. 5 Decomposition of 0.25 mM peroxynitrite at 25 °C and pH = 6.5 in 0.07 M phosphate buffer (I = 0.2 M) and simulation according to rate laws 2 and 3 with k_1 = 1.11 s^{-1} and k_3 = 1.35 s^{-1},[43] resulting in k_2 = 1163 M^{-1} s^{-1}. (a) Actual decay curve measured (black) and simulated (yellow); (b) residuals (green) of the model; (c) concentrations calculated for $ONOO^-$ (blue) and O_2NOO^- (red), [ONOOH] is not shown.

Table 2 Decomposition of 0.25 mM $ONOO^-$ at 25 °C in 0.07 M phosphate buffer, I = 0.2 M adjusted by $NaClO_4$, k_1 = 1.11 ± 0.01 s^{-1}, k_3 = 1.35 s^{-1},[43] n measurements. The error of 1 is based on all 27 measurements from pH 6.1 to 8.0 at the 95% confidence level

pH	First $t_{1/2}$/s	$k_2/(10^3\ M^{-1}\ s^{-1})$	n
5.3	0.69 ± 0.01	—	7
6.1	0.76 ± 0.04	0.9 ± 1.0	4
6.5	0.92 ± 0.03	1.3 ± 0.3	4
7.0	1.41 ± 0.02	1.7 ± 0.1	4
7.2	2.21 ± 0.06	1.1 ± 0.1	6
7.7	4.6 ± 0.1	1.4 ± 0.1	5
8.0	9.4 ± 0.1	1.7 ± 0.1	4
Over all pH values		1.3 ± 0.1	27

peroxynitrite. The first half-life of the absorbance at pH 6–8 can be calculated according to rate laws 2 and 3 with k_1 = 1.11 s^{-1}, k_2 = 1.3 × 10^3 M^{-1} s^{-1} and k_3 = 1.35 s^{-1} much more accurately than by a model based on a first-order decay only.

Decomposition of peroxynitrite in phosphate buffer and Tris buffer

The decomposition of peroxynitrite is decelerated by phosphate and accelerated by Tris: $t_{1/2}$ = 0.75–0.88 s in 0.1 M phosphate and 0.1 M Tris, $t_{1/2}$ = 1.33–1.42 s in 0.1 M phosphate

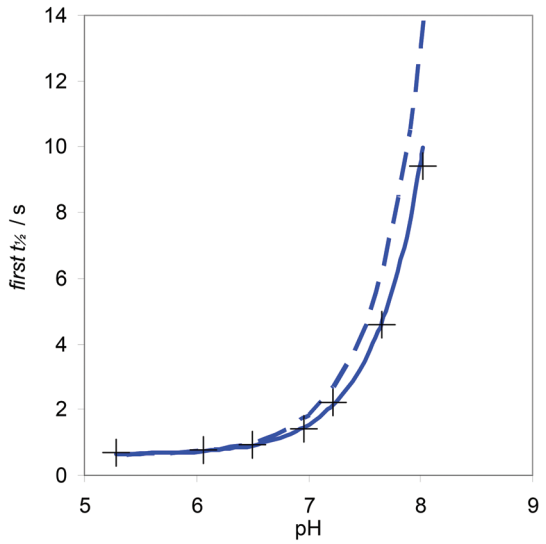

Fig. 6 Decomposition of 0.25 mM peroxynitrite at pH = 5.3, 6.1, 6.5, 7.0, 7.2, 7.7 and 8.05 in 70 mM phosphate buffer (I = 0.2 M). The first half-life of the absorbance measured (+) and calculated (blue lines) based on the best fit of two decomposition models: (1) (dashed line) according to isomerization only with k_1 = 1.11 s^{-1}; (2) (solid line) according to rate laws 2 and 3 with k_1 = 1.11 s^{-1}, k_2 = 1.3 × 10^3 M^{-1} s^{-1} and k_3 = 1.35 s^{-1}.

Table 3 Decomposition of 0.25 mM peroxynitrite at 25 °C and pH = 6.8 in 0.1 M Tris buffers (I = 0.2 M) at various phosphate concentrations. n, the number of determinations

[Phosphate]/M	First $t_{1/2}$/s	$k_2/(10^3\ M^{-1}\ s^{-1})$	n
0	0.65 ± 0.00	14 ± 2	2
0.001	0.68 ± 0.02	13 ± 1	5
0.005	0.69 ± 0.09	13 ± 4	3
0.025	0.73 ± 0.04	12 ± 3	3
0.1	0.91 ± 0.02	9.3 ± 0.4	6

Table 4 Decomposition of 0.25 mM peroxynitrite at 25 °C and pH = 6.8 in 0.1 M phosphate buffers (I = 0.2 M) at various Tris concentrations

[Tris]/M	k_2 [a]$/(10^3\ M^{-1}\ s^{-1})$	k_2 [b]$/(10^3\ M^{-1}\ s^{-1})$
0	1.3	1.2
1×10^{-4}	[c]	1.3
3×10^{-4}	1.3	1.5
1×10^{-3}	1.5	2.0
3×10^{-3}	2.4	2.8
0.01	3.7	4.4
0.03	5.1	5.2
0.1	8.0	9.4

Initial total peroxynitrite concentration: [a] 260 μM and [b] 340 μM. [c] Not determined.

only and $t_{1/2}$ = 0.63 s in 0.1 M Tris only (Tables 3 and 4, and Fig. 7).

Interestingly, up to a certain concentration, Tris shows no significant influence on the decay of peroxynitrite. However, this concentration decreases with increasing initial peroxynitrite concentration. We find that the measured first half-life

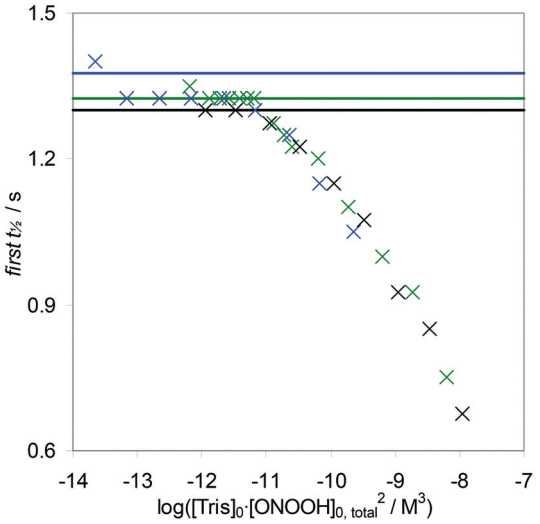

Fig. 7 Decomposition of 0.047 mM (blue), 0.25 mM (green) and 0.34 mM (black) peroxynitrite at pH = 6.8 in 0.1 M phosphate buffers with varied Tris concentrations. The solid horizontal lines indicate the first half-life of the absorbance of peroxynitrite in the absence of Tris. When $[Tris]_0 \cdot [ONOO^-]_{0,\,total}^2$ exceeds 6.3×10^{-12} M^3, Tris significantly catalyses the disproportionation.

of the absorbance of peroxynitrite correlates with $[Tris]_0 \cdot [ONOO^-]_{0,\,total}^2$: if $[Tris]_0 \cdot [ONOO^-]_{0,\,total}^2$ exceeds 6.3×10^{-12} M^3 ($1 \times 10^{-11.2}$ M^3), then Tris significantly accelerates the decomposition of peroxynitrite (Fig. 7).

Discussion

According to rate laws 2 and 3, absorption traces are fitted (*e.g.* Fig. 5) and values of the first half-life of the absorbance are simulated (Fig. 6) without a systematic error for the pH range 6–8. A model restricted to homolysis[37] does not simulate the decay of peroxynitrite in this pH range very well.

The first-order rate constant of the isomerization agrees with earlier results.

The disproportionation can be regarded as a two-step reaction: a reversible association and a subsequent irreversible conversion to the products:

$$ONOOH + ONOO^- \underset{k_{-6}}{\overset{k_6}{\rightleftharpoons}} [ONOOH \cdot ONOO^-]^{\neq} \overset{k_7}{\rightarrow} H^+ + 2NO_2^- + O_2$$

$$\frac{\partial[\text{products}]}{\partial t} = k_7[ONOOH \cdot ONOO^-] = \frac{k_6 k_7}{k_{-6} + k_7}[ONOOH][ONOO^-] = k_2[ONOOH][ONOO^-] \rightarrow k_2 = \frac{k_6 k_7}{k_{-6} + k_7} \quad (8)$$

Earlier estimates of the parameters of this sequence are listed in Table 5. The first two are in good agreement with the disproportionation rate constant determined here; however, the third estimate is higher.

Table 5 Rate constants of the decomposition of peroxynitrite into NO_2^- and O_2

k_6/(M^{-1} s^{-1})	k_{-6}/(s^{-1})	k_7/(s^{-1})	k_2/(M^{-1} s^{-1})	Source
		0.20 ± 0.01	(2.0 ± 0.1) × 10^3	Decay modelling[14]
2.5×10^5	25	0.2–0.3	(2–3) × 10^3	Decay modelling[36]
1.7×10^4	0.025	0.05	1.1×10^4	Decay modelling[55]
			(1.3 ± 0.1) × 10^3	This work

According to rate laws 2 and 3, the concentration of peroxynitrate reaches its concentration maximum *ca.* 1 s after the decay of peroxynitrite is initiated (Fig. 5c). After that peak concentration, the second-order disproportionation becomes negligible in comparison with first-order decay processes 1 and 3. Therefore, decay traces of peroxynitrite deviate from first-order kinetics in the first 1–2 s.[33]

The decomposition model according to reactions (1)–(3)§ and (9) fails to reproduce the Tris-dependent first half-life of the absorbance. It fits the absorption curves with a residual that indicates a systematic error that increases with the Tris concentration (not shown). Moreover, it results in k_2 values that increase non-linearly with the Tris concentration if the latter is higher than 10^{-4} M (Table 4). Saturation may cause a non-linear dependence. The accelerating effect of Tris will be addressed in a future publication.

We find that k_2 is one order of magnitude lower in phosphate buffer (this work: 1.3×10^3 M^{-1} s^{-1}) than in Tris buffer (this work: 9×10^3 M^{-1} s^{-1}, Gupta *et al.*:[38] 3×10^4 M^{-1} s^{-1}, both in 0.1 M Tris) and that 0.25 mM peroxynitrite decomposes in 0.1 M Tris buffer twice as fast as it does in 0.1 M phosphate buffer. Therefore, Tris accelerates the disproportionation of peroxynitrite and thereby increases k_2. Indeed, the peroxynitrate yield is, being dependent on the square of the initial peroxynitrite concentration, 40 times higher in Tris buffer than it is in phosphate buffer.[38] The observed rate of decay of peroxynitrite accelerates with increasing Tris concentration (Fig. 7). Furthermore, the first half-life of the absorbance correlates with the concentration product $[Tris]_0 \cdot [ONOO^-]_{0,\,total}^2$. The concentration product $[Tris] \cdot [ONOO^-]_{total}^2$ is likely part of the rate law of the additional Tris-dependent decomposition pathway. If the Tris concentration is high enough, this additional decomposition pathway contributes significantly to the overall decomposition. If Tris participates in the disproportionation according to reaction (9) and if $k_{2,\,in\ Tris} = k_2 + k_9 \cdot [Tris]$, then we obtain an estimate of k_9 = (8–29) × 10^3 M^{-2} s^{-1}:

$$ONOOH + ONOO^- + Tris \overset{k_9}{\rightarrow} O_2NOO^- + NO_2^- + TrisH^+ \quad (9)$$

It is likely that a more accurate decomposition model can be achieved by considering a chain of association equilibria that involve peroxynitrite and Tris.

Peroxyacids, in general, decompose in reactions that are first-order in both the acid and its conjugate base: typically with rate constants of 1×10^{-3}–1×10^{-1} M^{-1} s^{-1}.[56–59] These rate constants are much smaller than those found for

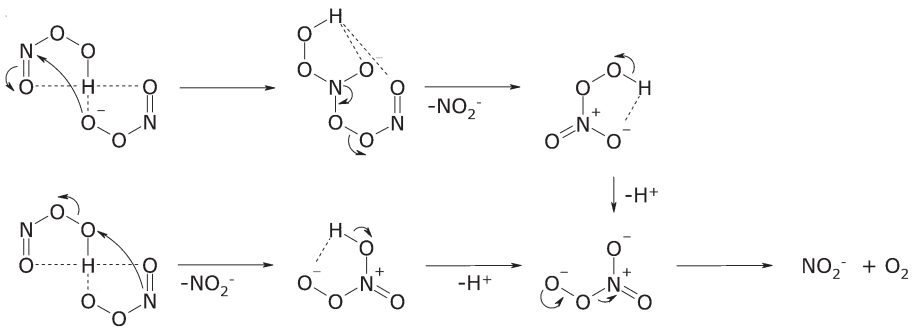

Scheme 2

peroxynitrite (1.3×10^3–3×10^4 M^{-1} s^{-1}). However, in contrast to other peroxyacids, the atom attached to the OOH group of peroxynitrite has a lone pair that allows additional reactions – electrophilic attack and oxidative addition – that may allow faster decomposition (Scheme 2).

At peroxynitrite concentrations $>10^{-4}$ M, but at lower concentration in the presence of Tris, disproportionation of peroxynitrite in samples competes with reactions of peroxynitrite with target molecules and produces peroxynitrate that is an artificial reactive intermediate.

Acknowledgements

We thank the SNF and the ETH Zurich for financial support.

References

1 N. G. Connelly, T. Damhus, R. M. Hartshorn and A. T. Hutton, *Nomenclature of Inorganic Chemistry. IUPAC Recommendations 2005*, 2005.
2 W. H. Koppenol, *Pure Appl. Chem.*, 2000, **72**, 437–446.
3 N. V. Blough and O. C. Zafiriou, *Inorg. Chem.*, 1985, **24**, 3502–3504.
4 T. Nauser and W. H. Koppenol, *J. Phys. Chem. A*, 2002, **106**, 4084–4086.
5 H. Botti, M. Möller, D. Steinmann, T. Nauser, W. H. Koppenol, A. Denicola and R. Radi, *J. Phys. Chem. B*, 2010, **114**, 16584–16593.
6 S. Moncada, M. W. Radomski and R. M. J. Palmer, *Biochem. Pharmacol.*, 1988, **37**, 2495–2501.
7 J. B. Hibbs, R. R. Taintor, Z. Vavrin and E. M. Rachlin, *Biochem. Biophys. Res. Commun.*, 1988, **157**, 87–94.
8 M. R. Green, H. A. O. Hill, M. J. Okolow-Zubkowska and A. W. Segal, *FEBS Lett.*, 1979, **100**, 23–26.
9 R. J. Gryglewski, R. M. J. Palmer and S. Moncada, *Nature*, 1986, **320**, 454–456.
10 T. B. McCall, N. K. Boughton-Smith, R. M. J. Palmer, B. J. R. Whittle and S. Moncada, *Biochem. J.*, 1989, **261**, 293–296.
11 Y. Xia, V. L. Dawson, T. M. Dawson, S. H. Snyder and J. L. Zweier, *Proc. Natl. Acad. Sci. U. S. A.*, 1996, **93**, 6770–6774.
12 J. S. Beckman, T. W. Beckman, J. Chen, P. A. Marshall and B. A. Freeman, *Proc. Natl. Acad. Sci. U. S. A.*, 1990, **87**, 1620–1624.
13 P. Pacher, J. S. Beckman and L. Liaudet, *Physiol. Rev.*, 2007, **87**, 315–424.
14 R. Kissner, T. Nauser, P. Bugnon, P. G. Lye and W. H. Koppenol, *Chem. Res. Toxicol.*, 1997, **10**, 1285–1292.
15 M. Anbar and H. Taube, *J. Am. Chem. Soc.*, 1954, **76**, 6243–6247.
16 J. D. Ray, *J. Inorg. Nucl. Chem.*, 1962, **24**, 1159–1162.
17 W. H. Koppenol, J. J. Moreno, W. A. Pryor, H. Ischiropoulos and J. S. Beckman, *Chem. Res. Toxicol.*, 1992, **5**, 834–842.
18 C. Kurz, X. Zeng, S. Hannemann, R. Kissner and W. H. Koppenol, *J. Phys. Chem. A*, 2005, **109**, 965–969.
19 W. H. Koppenol, P. L. Bounds, T. Nauser, R. Kissner and H. Ruegger, *Dalton Trans.*, 2012, **41**, 13779–13787.
20 W. G. Keith and R. E. Powell, *J. Chem. Soc. A*, 1969, 90–90.
21 S. V. Lymar and J. K. Hurst, *J. Am. Chem. Soc.*, 1995, **117**, 8867–8868.
22 A. Denicola, B. A. Freeman, M. Trujillo and R. Radi, *Arch. Biochem. Biophys.*, 1996, **333**, 49–58.
23 D. M. Stanbury, *Adv. Inorg. Chem.*, 1989, **33**, 69–138.
24 R. E. Huie, C. L. Clifton and P. Neta, *Radiat. Phys. Chem.*, 1991, **38**, 477–481.
25 S. V. Lymar, Q. Jiang and J. K. Hurst, *Biochemistry*, 1996, **35**, 7855–7861.
26 M. S. Ramezanian, S. Padmaja and W. H. Koppenol, *Chem. Res. Toxicol.*, 1996, **9**, 232–240.
27 J. N. Lemercier, S. Padmaja, R. Cueto, G. L. Squadrito, R. M. Uppu and W. A. Pryor, *Arch. Biochem. Biophys.*, 1997, **345**, 160–170.
28 F. Barat, L. Gilles, B. Hickel and J. Sutton, *J. Chem. Soc. A*, 1970, 1982–1986.
29 T. Løgager and K. Sehested, *J. Phys. Chem.*, 1993, **97**, 6664–6669.
30 B. Alvarez and R. Radi, First Int. Conf. Chemistry and Biology of Peroxynitrite, Ascona, 1997, 2–2.
31 W. H. Koppenol and R. Kissner, *Chem. Res. Toxicol.*, 1998, **11**, 87–90.

32 P. Maurer, C. F. Thomas, R. Kissner, H. Rüegger, O. Greter, U. Röthlisberger and W. H. Koppenol, *J. Phys. Chem. A*, 2003, **107**, 1763–1769.
33 J. S. Beckman, H. Ischiropoulos, L. Zhu, M. van der Woerd, C. D. Smith, J. Chen, J. Harrison, J. C. Martin and M. Tsai, *Arch. Biochem. Biophys.*, 1992, **298**, 438–445.
34 R. Radi, J. S. Beckman, K. M. Bush and B. A. Freeman, *Arch. Biochem. Biophys.*, 1991, **288**, 481–487.
35 S. Pfeiffer, A. C. F. Gorren, K. Schmidt, E. R. Werner, B. Hansert, D. S. Bohle and B. Mayer, *J. Biol. Chem.*, 1997, **272**, 3465–3470.
36 R. Kissner and W. H. Koppenol, *J. Am. Chem. Soc.*, 2002, **124**, 234–239.
37 M. Kirsch, H.-G. Korth, A. Wensing, R. Sustmann and H. de Groot, *Arch. Biochem. Biophys.*, 2003, **418**, 133–150.
38 D. Gupta, B. Harish, R. Kissner and W. H. Koppenol, *Dalton Trans.*, 2009, 5730–5736.
39 T. Løgager and K. Sehested, *J. Phys. Chem.*, 1993, **97**, 10047–10052.
40 S. Goldstein and G. Czapski, *Inorg. Chem.*, 1997, **36**, 4156–4162.
41 D. S. Bohle, B. Hansert, S. C. Paulson and B. D. Smith, *J. Am. Chem. Soc.*, 1994, **116**, 7423–7424.
42 S. Miyamoto, G. E. Ronsein, T. C. Corrêa, G. R. Martinez, M. H. G. Medeiros and P. Di Mascio, *Dalton Trans.*, 2009, 5720–5729.
43 S. Goldstein, G. Czapski, J. Lind and G. Merényi, *Inorg. Chem.*, 1998, **37**, 3943–3947.
44 W. H. Koppenol, *Inorg. Chem.*, 2012, **51**, 5637–5641.
45 W. H. Koppenol, D. M. Stanbury and P. L. Bounds, *Free Radical Biol. Med.*, 2010, **49**, 317–322.
46 D. D. Wagman, W. H. Evans, V. B. Parker, R. H. Schumm, I. Halow, S. M. Bailey, K. L. Churney and R. L. Nuttal, *J. Phys. Chem. Ref. Data*, 1982, **11**(Suppl. 2), 37–38.
47 P. Warneck and C. Wurzinger, *J. Phys. Chem.*, 1988, **92**, 6278–6283.
48 M. Kirsch, E. E. Lomonosova, H.-G. Korth, R. Sustmann and H. de Groot, *J. Biol. Chem.*, 1998, **273**, 12716–12724.
49 S. Kapiotis, M. Hermann, I. Held, A. Mühl and B. Gmeiner, *FEBS Lett.*, 1997, **409**, 223–226.
50 D. Tsikas, K. Denker and J. C. Frölich, *J. Chromatogr., A*, 2001, **915**, 107–116.
51 E. Pollet, J. A. Martínez, B. Metha, B. P. Watts Jr. and J. F. Turrens, *Arch. Biochem. Biophys.*, 1998, **349**, 74–80.
52 D. S. Bohle, P. A. Glassbrenner and B. Hansert, *Methods Enzymol.*, 1996, **269**, 302–311.
53 P. Latal, R. Kissner, D. S. Bohle and W. H. Koppenol, *Inorg. Chem.*, 2004, **43**, 6519–6521.
54 R. M. Smith and A. E. Martell, *Critical Stability Constants: Volume 4: Inorganic Complexes*, 1976.
55 R. Kissner, T. Nauser, C. Kurz and W. H. Koppenol, *IUBMB Life*, 2003, **55**, 567–572.
56 D. F. Evans and M. W. Upton, *J. Chem. Soc., Dalton Trans.*, 1985, 1151–1153.
57 J. F. Goodman, P. Robson and E. R. Wilson, *Trans. Faraday Soc.*, 1962, **58**, 1846–1851.
58 E. Koubek, M. L. Haggett, C. J. Bataglia, K. M. Ibne-Rasa, H. Y. Pyun and J. O. Edwards, *J. Am. Chem. Soc.*, 1963, **85**, 2263–2268.
59 Z. Yuan, Y. Ni and A. R. P. van Heiningen, *Can. J. Chem. Eng.*, 1997, **75**, 37–41.